Trends in Ln(III) Sorption to Quartz Assessed by Molecular Dynamics Simulations and Laser Induced Flourescence Studies

ARTICLE *in* THE JOURNAL OF PHYSICAL CHEMISTRY C · NOVEMBER 2011

Impact Factor: 4.77 · DOI: 10.1021/jp204633g

6 AUTHORS, INCLUDING:

Zheming Wang
Pacific Northwest National Laboratory
181 PUBLICATIONS **3,311** CITATIONS
SEE PROFILE

Nathalie A Wall
Washington State University
42 PUBLICATIONS **253** CITATIONS
SEE PROFILE

Aurora E Clark
Washington State University
80 PUBLICATIONS **1,300** CITATIONS
SEE PROFILE

THE JOURNAL OF PHYSICAL CHEMISTRY C

ARTICLE

pubs.acs.org/JPCC

Trends in Ln(III) Sorption to Quartz Assessed by Molecular Dynamics Simulations and Laser-Induced Fluorescence Studies

Jadwiga Kuta,[†] Matthew C. F. Wander,[†,§] Zheming Wang,[*,‡] Siduo Jiang,[‡] Nathalie A. Wall,[*,†] and Aurora E. Clark[*,†]

[†]Department of Chemistry, Washington State University, Pullman, Washington 99164, United States

[‡]Fundamental and Computational Science Directorate, Pacific Northwest National Laboratory, Richland, Washington 99352, United States

Supporting Information

ABSTRACT: Molecular dynamics simulations were performed to examine trends in trivalent lanthanide [Ln(III)] sorption to ≡SiOH^0 and ≡SiO$^-$ sites on the 001 surface of α-quartz across the 4f period. Complementary laser-induced fluorescence studies examined Eu(III) sorption to α-quartz at a series of ionic strengths from 1×10^{-4} M to 0.5 M such that properties of the surface-sorbed species could be extrapolated to zero ionic strength, the conditions under which the simulations are performed. Such extrapolation allows for a more direct comparison of the data and enables a molecular understanding of the surface-sorbed species and the role of the ion surface charge density upon the interfacial reactivity. Potential of mean force molecular dynamics as well as simulations of presorbed Ln(III) species agrees with the spectroscopic study of Eu(III) sorption, indicating that strongly bound inner-sphere complexes are formed upon sorption to an ≡SiO$^-$ site. The coordination shell of the ion contains 6−7 waters of hydration, and it is predicted that surface silanol OH groups transfer from the quartz to the inner coordination shell of Eu(III). Molecular simulations predict less-strongly bound inner-sphere species in early lanthanides and more strongly bound species in late lanthanides, following trends in the surface charge density of the 4f ions. Hydroxyl ligands that derive from the surface silanol groups are consistently observed to bind in the inner coordination shell of surface-sorbed inner-sphere Ln(III) ions, provided that the ion is able to migrate within 2.0−3.0 Å of the plane formed by the silanol O atoms (~3.5 Å from an individual ≡SiO$^-$ group). Sorption to a fully protonated quartz surface is not predicted to be favorable by any Ln(III), except perhaps Lu. The present work demonstrates a combined theoretical and experimental approach in the prediction of the fate of trivalent radioactive contaminants at temporary and permanent nuclear waste storage sites.

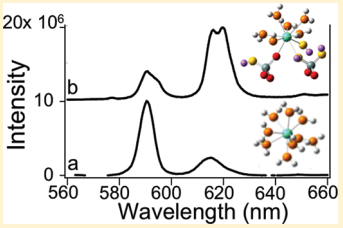

INTRODUCTION

Trivalent lanthanides [Ln(III)] and actinides [An(III)] are present in nuclear wastes that have not been reprocessed, and Ln(III) are commonly considered chemical analogs for An(III), due to the similar bonding character of the trivalent f-block elements.[1,2] Moreover, Ln(III) are less susceptible to solution phase and surface oxidation and reduction (redox) reactions that can complicate chemical interpretation of surface-bound species. As such, the geochemical behavior of Ln(III) has been extensively investigated with respect to the performance assessment of nuclear waste repositories and remediation of sites contaminated with both Ln and An.[3,4] Evidence suggests that oxide minerals are the key sorbents responsible for controlling the fate and transport of Ln elements in natural systems,[5] and although significant advances have been made in our understanding of their reactivity with oxides, major deficiencies remain. Although batch sorption and column experiments provide useful information on the effects of solution chemistry and mineral properties on Ln sorption behavior, they describe only the macroscopic aspects of ion interactions with the mineral surface and give no direct information on the structure and local chemical environment of sorbed species. More information can be gleaned from surface complexation models (SCMs) that use thermodynamic and kinetic databases combined with mathematical algorithms to fit metal sorption experimental data.[6−8] However, the primary limitation of SCMs is that the site-specific structural parameters for these models are too strongly correlated to small changes in pH and other global paramaters, thus reducing or eliminating their geochemical value.

In recent years, molecular spectroscopy has emerged as a vital component to elucidate molecular scale structures sorbed to mineral surfaces, providing insight into the types of surface complexes and precipitations formed as a function of the metal ion, mineral surface, pH, surface coverage, etc.[9] Molecular simulations have also proven a useful complement to sorption and spectroscopic experiments. In this case, the sorption behavior of specific ions can be studied directly through the simulations of realistic models of molecular complexes at mineral surfaces.[10] However, these computational studies typically do not account for the influence of ionic strength (I), are performed without consideration of pH, and lack meaningful comparison with experimental observations under similar conditions. Thus, the

Received: May 18, 2011
Revised: September 5, 2011
Published: September 15, 2011

Table 1. Structural and Statistical Data for Ln(III) in SPC Water[a]

ion	fit	$\langle r_{min}\rangle_{DFT}$	$\langle r_{Ln-OH_2}\rangle_{MD}$	$\langle r_{Ln-OH_2}\rangle_{exp}$	CN	CN_{exp}	D_M
$La(H_2O)_9^{3+}$	gas	2.62	2.55	2.54[b], 2.56[c], 2.58[d]	9.05	9.2[b], 9[c], 9.13[d]	0.849 ± 0.014
	PCM	2.57	2.38		8.95		0.519 ± 0.012
$Eu(H_2O)_9^{3+}$	gas	2.51	2.52	2.43[b,e]	9.02	9.3[b], 8.6[e]	0.328 ± 0.008
$Lu(H_2O)_8^{3+}$	gas	2.37	2.18	2.31[e], 2.34[f]	8.11	7.7[e], 7.97[f]	0.978 ± 0.019
	PCM	2.32	2.23		8.02		0.449 ± 0.016

[a] The average $Ln-OH_2$ distances according to DFT, and using the fitted force field for MD simulation compared with experimental values in angstroms, along with the metal ion coordination number in the first hydration shell (CN), and the diffusion coefficient, D_M (10^{-5} cm^2/s), are presented. [b] Ref 40. [c] Ref 48. [d] Ref 49. [e] Ref 50. [f] Ref 38.

resulting conclusions are prone to errors because no real chemical system exists with zero ionic strength, which is well-known to affect chemical and geochemical metal behaviors.[11,12] Ln mobility can increase under acidic conditions and with increasing ionic strength,[13] because metal speciation depends strongly on solution pH and the surface charge becomes more negative with increasing pH for most natural soil and sediment sorbents.[14] Unfortunately, the inclusion of such effects in modeling exercises is not straightforward. To improve the effectiveness of theoretical simulation methods, it is desirable to determine the sorption properties of Ln(III) under experimental conditions that closely mimic the environments within molecular simulations, enabling detailed comparisons of experimental and theoretical data in a unique and rigorous way.

In this work, classical molecular dynamics (MD) simulations have been applied to examine the chemical behavior of Ln(III) in aqueous solution as well as Ln(III) sorption to ≡$SiOH^0$ and ≡SiO^- sites on the 001 surface of α-quartz. Eu(III) sorption to a sample of α-quartz has been experimentally determined at different ionic strengths using spectroscopic techniques, allowing the extrapolation of key data to zero ionic strength, the conditions employed in the MD simulations. Further, experimental Eu(III) sorption studies were performed at pH 7 and 9 to compare experimental and simulation data for Eu sorption to different potential surface sites.

COMPUTATIONAL METHODS

Force Field Development. Prior to MD simulation of aqueous Ln(III), classical potentials that describe the $Ln-OH_2$ interaction were developed to be used with the nonpolarized SPC water model. To ensure that the trends observed in the sorption simulations are robust and generalizable, two sets of interaction potentials have been generated on the basis of fitting to either gas- or solution-phase dissociation of H_2O from $Ln(H_2O)_9^{3+}$ and $Ln(H_2O)_8^{3+}$ species. This process first consisted of obtaining the ab initio optimized geometries of $La(H_2O)_9^{3+}$, $Eu(H_2O)_9^{3+}$, and $Lu(H_2O)_8^{3+}$, as in our prior work,[15] using B3LYP DFT[16,17] with the RSC28 core potential and basis set for Ln(III) and the aug-cc-pVDZ basis on O and H atoms.[18−20] Optimizations were performed in the gas phase using NWChem[21] as well as in a polarized continuum model (PCM) that mimics the effect of the bulk solvent dielectric using an UAKS cavity[22] in Gaussian 03.[23] Due to wave function convergence issues, the PCM optimization of $Eu(H_2O)_9^{3+}$ was not performed. The resulting coordination environments and gas phase metal−water bond lengths agree well with experiment (within ∼0.05 Å), and use of a PCM contracts the r_{Ln-OH_2} bond lengths by ∼0.05 Å, leading to near perfect agreement (Table 1).

A water dissociation potential energy surface (PES) was then created by stretching one of the equatorial $Ln-OH_2$ bond distances in the tricapped trigonal biprismatic $Ln(H_2O)_9^{3+}$, or one of the eight equivalent $Ln-OH_2$ distances in the square antiprismatic $Ln(H_2O)_8^{3+}$, keeping all other geometrical parameters fixed. Geometric relaxation was not allowed along the water dissociation surface because it introduces higher-body effects that cannot be reproduced by a simple Lennard-Jones potential. The resulting data set consisted of 41 gas phase or PCM data points 0.05 Å apart within the range of −1.0 to +1.0 Å around the minimum, r_{min}, of the DFT PES for each system (Table 1).

Finally, fitting of the $Ln-OH_2$ potential to the ab initio gradients of the H_2O dissociation PES was performed according to our earlier work[24] using the ForceFit program.[25] The specific analytic expressions for the $La-OH_2$ interatomic potential are based upon the nonbonding interaction terms (and charges) found in the SPC water model,[26−28] using a formal charge of 3+ on the metal. The $Ln-OH_2$ interaction was described using a Lennard-Jones (LJ) model plus Coulomb function. Similar fitting strategies have been employed in prior work to reproduce a variety of properties of aqueous Ln(III) using different water models.[29−31]

To test the fitted $Ln-OH_2$ LJ potentials (Table S1 in the Supporting Information), MD simulations of Ln^{3+} were first performed in a 40 Å × 40 Å × 40 Å SPC water box containing 2039 H_2O molecules using DL_POLY 3.10.0.[32] The complete simulation protocol is presented in the Supporting Information. The quality of the $Ln-OH_2$ interaction potential was assessed through comparison of the radial distribution functions, average coordination number about the ion, and diffusion coefficient of the ion to experimental data.

MD Simulation of Ln^{3+} Sorption to Quartz. The construction and simulation of the α-quartz simulation cell was performed as in our prior work and is described in detail within the Supporting Information.[33] The MD simulations were performed using LAMMPS[34,35] with the CLAYFF force field,[36] which uses a flexible SPC water model.[26−28] Our previous studies have indicated excellent reproduction of the properties of interfacial water on quartz using this model; however, surface-binding energies of ions on the surface may be underestimated, given the lack of any polarization affects within the water model. The complete simulation protocol is presented in the Supporting Information. To investigate ion sorption to α-quartz, two types of simulations were performed: (1) potential of mean force (PMF), which calculates the free energy of ion sorption along a prescribed reaction pathway to either a protonated (≡$SiOH^0$) or deprotonated (≡SiO^-) surface site (the rest of the surface being fully protonated), and (2) equilibration of a presorbed Ln(III) ion to both an ≡$SiOH^0$ and ≡SiO^- group on the fully protonated

001 surface. Potential of mean force simulations were performed using a modified version of the LAMMPS code wherein the ion was held at a fixed z distance above the surface. At each point along the sorption reaction coordinate, 150 000 steps of equilibrations with a 1 fs time step were performed. The forces were collected after 500 000−800 000 timesteps, with the program exiting when the total standard deviation in forces is $<10^{-3}$.

The first data point placed the Ln^{3+} ion 8.0 Å above the average plane formed by the surface O atoms and brought the ion toward that plane in increments of 0.20 Å until a distance of 1.0 Å was obtained (at an average $Ln^{3+}\cdots O-Si$ distance of 2 Å). Inspection of the free energy profiles prompted equilibration simulations in which the ion was placed at one of three distances from the surface that represent reactivity within different energy regimes should environmental or surface conditions drive the ion to different positions on the sorption potential energy surface (e.g., higher temperatures, step edges, defect sites, etc.). In the first equilibration, the ion was placed 1.0 Å above the average plane formed by the surface silanol O atoms, at an average $Ln^{3+}\cdots O-Si$ distance of 2 Å, and constrained at this distance, being allowed to move in the xy plane, parallel to the surface. After 1000 timesteps of minimization, 1 000 000 timesteps of the constrained simulation followed with a time step of 1 fs (1 ns total), after which the constraint was removed, and the system was allowed to fully equilibrate for another 3 ns in the NVE ensemble at 300 K, with an Ewald precision of 10^{-8}. Statistical data was collected for the final nanosecond only. Two other equilibration simulations following the same protocol were performed; however, with the initial distance of the ion at 2.0 and 3.0 Å above the average plane formed by the surface silanol O-atoms, respectively.

EXPERIMENTAL SECTION

Quartz Sample Preparation and Sorption Measurements. Quartz samples of "Min-U-Sil 30" were obtained from the Pennsylvania Glass & Sand Company and purified according to Kohler et al.[37] The resulting solid was filtered in suspension over a 0.45 μm pore size nylon filter, dried, and kept in a desiccator when not in use. Powder X-ray diffraction analysis ensured the identity of the final product as α-quartz, as in prior study of Minusil-5.[38] The samples used to study Eu(III) sorption on quartz at pH 7 were prepared as follows: 1.0 g of purified quartz was added to 160 mL of DDI water and 3×10^{-7} mol of $Eu(ClO_4)_3$, the pH of the suspension was adjusted with dilute $HClO_4$ and NaOH to 7.0, and more DDI water was added to obtain a final sample volume of 200 mL. The resulting suspension was allowed to equilibrate in atmospheric condition of CO_2 for 24 h, after which 20 mL was sampled as one with the lowest ionic strength that was calculated by the added electrolytes and any dissolved bicarbonate. Afterward, increasing amounts of $NaClO_4$ solution were added to reach predefined ionic strengths. At each ionic strength, a 20 mL aliquot of the suspension was sampled. Minor pH adjustments of the suspension were performed with dilute NaOH and $HClO_4$ solution to reach pH 7.0 ± 0.1. All suspension samples were then allowed to equilibrate for an additional 24 h under slow shaking. Upon centrifugation, the resulting supernatant was sampled for the final pH measurement and Eu analysis by ICP-OES. The solid paste was transferred to a 2 mm × 4 mm × 25 mm quartz cuvette for fluorescence analysis. The samples for Eu(III) sorption on quartz at pH 9 were prepared in a similar way except that the suspension pH was adjusted by Na_2CO_3 and $NaHCO_3$ solutions. The calculated ionic strength included contributions from carbonate and bicarbonate. The ionic strengths, final solution pH, and the amount of Eu adsorbed on the quartz are listed in Table S2 in the Supporting Information.

Spectroscopic Measurements. The fluorescence emission spectra of Eu(III) adsorbed on quartz were recorded by excitation at 394 nm, corresponding to the $^7F_0 \rightarrow {}^5L_6$ electronic transition, with the frequency-doubled output of a Spectra Physics MOPO-730 running at 10 Hz with a pulse width of typically ~20 ns. The resulting fluorescence was collected at 85° with respect to the excitation beam by a 2 in diameter f/3 fused-silica lens, focused by a 2 in f/4 fused-silica lens into the entrance slit of a 0.3 m focal length Acton SpectroPro 300i double monochromator spectrograph and recorded by a thermoelectrically cooled Princeton Instruments PIMAX time-gated, intensified CCD camera that was triggered by the delayed output of the laser pulse and controlled by WinSpec data acquisition software. The fluorescence lifetime of the Eu(III) samples were recorded by diverting the emitted light into a CVI model CM110 monochromator and detected by a Hamamatsu R928 photomultiplier tube (PMT). The fluorescence intensity signal from the PMT was amplified and recorded with a Tektronix TDS 754A digital oscilloscope. Fluorescence spectral and lifetime analysis were performed using a commercial software, IGOR, from Wavemetrix.

RESULTS AND DISCUSSION

MD of Ln(III) Ions in Water. Previous MD studies on $Ln(III)_{aq}$ have established the average geometric structure as well as ion diffusion coefficients and residence times of H_2O within the first hydration shell. The correct classical interatomic potential must capture the essential changes in coordination, diffusion coefficients, etc. across the series that arise from the contraction of the ionic radii from 1.16 Å in La(III) to 0.98 Å in Lu(III).[39] Specifically, the hydration coordination number (CN) of Ln(III) changes along the period, with early elements having CN = 9, while equilibrium is established between CN = 9 and CN = 8 in the middle of the series, and late Ln(III) have CN = 8.[40−44] The literature is mixed regarding the best analytic expressions to describe the $Ln-OH_2$ interaction; however, given the lack of polarizable water models available within the LAMMPS software, a nonpolarizable $Ln-OH_2$ interaction based upon the flexible SPC water model is used here.

As illustrated in Table 1, fitting to the water dissociation PES obtained in either the gas or solution phases yields the correct trends in CN and r_{Ln-OH_2} bond lengths across the Ln(III) series. The gas phase fits result in average $Ln-OH_2$ bond lengths that are within 0.1 Å of experimental data, whereas the solution-phase fits are typically 0.2 Å too short. The calculated diffusion coefficients (D_M) for Ln(III) ions in this work are all within the correct order of magnitude of the known experimental values, and some of the potentials reproduce the appropriate trends across the 4f block. According to open-end-capillary experiments, D_M decreases slightly across the series from 0.619×10^{-5} cm^2/s for La(III) to 0.578×10^{-5} cm^2/s for Tm(III).[45,46] The decrease in D_M is likely due to the increase in surface charge density of the ion across the period, which enhances polarization across hydration shells, causing the ion to "drag" more water molecules during diffusion. Prior MD simulations using polarizable $La-OH_2$ potentials were unable to reproduce this trend, with a calculated D_M of 0.35×10^{-5} cm^2/s for Nd(III) and Gd(III) and a D_M of 0.44×10^{-5} cm^2/s

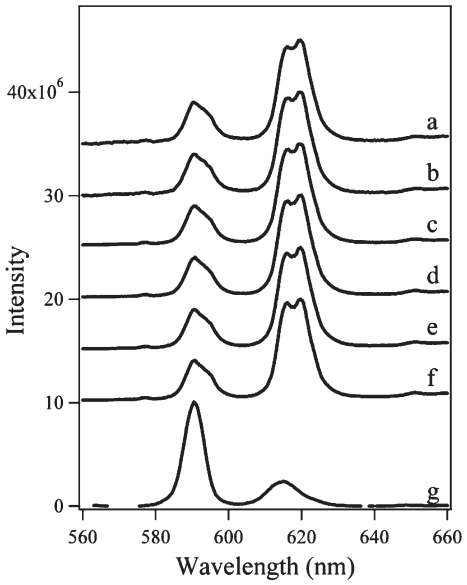

Figure 1. Fluorescence spectra of Eu(III) adsorbed on quartz. [Quartz] = 5 g/L; [Eu(III)] = 1.5 × 10^{-6} M. pH = 7; I = 0.01 M ($NaClO_4$). λ_{ex} = 394 nm. Trace a: steady-state spectra; traces b−f: time-resolved spectra with time delays of 0 (b), 0.1 (c), 0.2 (d), 0.3 (e), and 0.4 ms (f). The gatewidth was 0.1 ms. For comparison, the spectra of uncomplexed aqueous Eu(III) (g) is also shown. The spectra intensity were normalized and offset along the *Y*-axis for clarity.

for Yb(III).[47] Within this work, potentials derived from the gas-phase DFT data predict a similar, small increase in D_M (Table 1).

Floris et al. investigated whether the computed increase in D_M for polarized Ln−OH_2 potentials may be the result of inaccurate computation of D_M; however, use of macroscopic electrohydrodynamic theory did not improve their results. Interestingly, fits of the Ln−OH_2 potential to the DFT PCM data yields remarkably good agreement with experimental data, mirroring the small decrease as one goes from La(III) (D_M = 0.519 × 10^{-5} cm^2/s) to Lu(III) (D_M = 0.449 × 10^{-5} cm^2/s). This indicates that the quality of the ab initio data used in the fit has a significant impact upon D_M, but not as large upon structural characteristics such as hydration coordination number and Ln−OH_2 bond lengths. In combination with the structural information presented above, this is a good indication that the interatomic potentials derived in this work capture the essential physics of trivalent Ln(III) so as to yield chemically correct results for the structural aspects of ion sorption behavior that are reported in this work.

Sorption and LIF Studies of Eu(III) on Quartz. The adsorption of Eu(III) on quartz spanned 58−100% at pH 7.0 and 21−59% at pH 9.0, between the ionic strengths 5 × 10^{-4} and 0.5 M (Table S2 in the Supporting Information). The lower sorption at pH 9, compared with pH 7, is due to the predominance of the aqueous phase anionic $Eu(CO_3)_2^-$ species at high pH, and $Eu(OH)^{2+}$ is the major species at pH 7 under atmospheric conditions of CO_2, as calculated using the latest Am(III) thermodynamic data.[51] Eu(III) adsorbed on quartz displayed a series of emission bands corresponding to the $^5D_0 \rightarrow {}^7F_j$ (j = 0, 1, 2, ..., 6) transitions.[52,53] Both the steady-state (trace a, Figure 1) and the time-resolved fluorescence spectra at different delay times (traces b−f, Figure 1) closely resemble each other, indicating the formation of a unique surface complex or a limited number of similar surface complexes on quartz. These spectra are

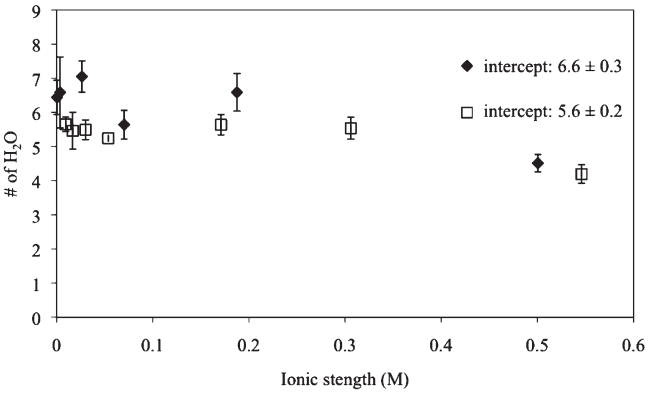

Figure 2. Plots of hydration number as a function of ionic strength at pH 7 (♦) and 9 (□).

significantly different from that of aqueous Eu(III) (trace g, Figure 1), as shown by the shift in the spectral maximum from 615 nm for aqueous Eu(III) to ∼619 nm for Eu(III) sorbed on quartz and the large increase in the spectral intensity of the 619 nm band relative to the 592 nm band. For Eu(III), both the spectral intensity and the position of the $^5D_0 \rightarrow {}^7F_2$ transition (615 nm) are sensitive to its coordination environment. It gains intensity and shifts to longer wavelength upon ligand complexation.[50,54,55] For aqueous Eu(III) ion, the band at 615 nm is less than half the intensity of the band at 592 nm. However, for complexed Eu(III), the 615 nm band can be several times more intense than the 592 nm band.[56] The present results clearly indicate formation of strong, inner-sphere Eu (III) surface complexes on quartz.[55,57,58]

The fluorescence decays of Eu(III) sorbed on quartz can be fitted by two exponential functions: a slower decay with a decay constant between 4.49 and 7.82 ms^{-1} (Figure S1 and Table S3 in the Supporting Information) and a fast decay with a decay constant of ∼60 ms^{-1} as compared with a fluorescence decay constant of the fully hydrated aqueous Eu(III) of 8.55 ms^{-1}.[59] For Eu(III) in aqueous solution, the major cause of the fluorescence decay is the O−H vibrators of the inner-sphere water or hydroxyl groups.[57,60] Therefore, the slower fluorescence decays reflects the displacement of the inner-sphere hydration waters of the aqueous Eu(III) upon sorption on the quartz surface. Using the linear relationship between the fluorescence decay constant and number of Eu(III) inner-sphere water molecules,

$$n_{H_2O} = 1.07k_{H_2O} - 0.7 \quad (1)$$

where k_{H_2O} is the measured fluorescence decay constants of Eu(III) (in ms^{-1}) and n_{H_2O} is the number of water molecules in the inner coordination sphere of Eu(III).[60] The number of water molecules remaining in the surface Eu(III) complexes was calculated to be 4.5−7.5 at pH 7 and 4.2−5.7 at pH 9 (Table S2 in the Supporting Information). Plots of the number of inner-sphere waters vs ionic strength showed that the number of inner-sphere water decreases as ionic strength increases (Figure 2). From the intercepts of the linear fits, the number of inner-sphere waters of surface-sorbed-Eu(III) at zero ionic strength were found to be 6.6 ± 0.3 at pH 7.0 and 5.6 ± 0.2 at pH 9.0, respectively. The results of less than seven inner-sphere waters in the adsorbed Eu(III) suggested that an additional ligand, such as hydroxyl (at pH 7) or carbonate (at pH 9), is involved in the surface complexes, leading to formation of ternary surface complexes. The observation of a fast fluorescence decay component (∼ 60 ms^{-1}) likely indicates that partial Eu(III)

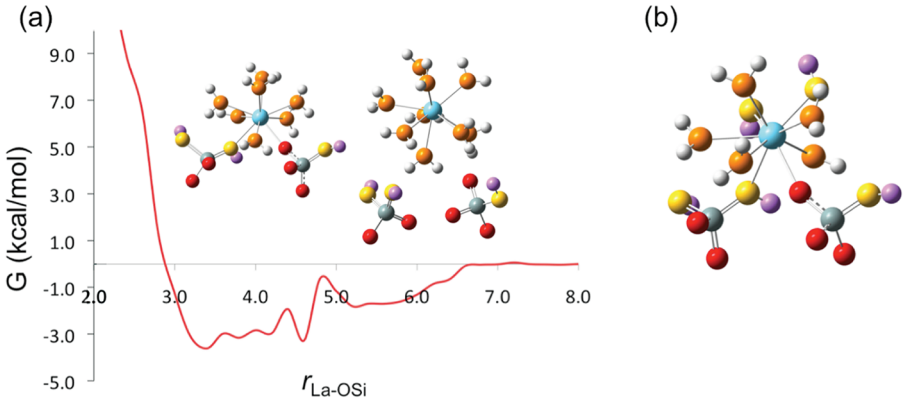

Figure 3. (a) PMF free-energy profile for La(III) sorption to quartz using the La−OH_2 interaction potential derived from gas phase DFT data, with structures of inner- and outer-sphere species inset. (b) Snapshot of sorbed La(III) on the surface of quartz from equilibrium simulation at an initial distance of 2.0 Å from the plane of the surface silanol O atoms. Si atoms colored gray; bridging O atoms are red; hydroxyl O atoms, yellow; hydroxyl H atom, pink; water O atoms are orange; water H atoms, white.

hydrolysis/precipitation or multinuclear complexes with oligomeric/polymeric silicates might have occurred, resulting in the formation of precipitated or multinuclear oligomeric surface species in which the short inter-Eu(III) distance causes effective fluorescence quenching and, thus, a large fluorescence decay rate.[61] A detailed investigation of this Eu(III) species is beyond the scope of this work.

MD Simulation of Ln(III) Sorption to Quartz. Since quartz has a point-of-zero charge of ∼2.3,[62] the presence of ≡$SiOH_2^+$ surface sites is negligible at pH 7−9. Instead, the surface is dominated by ≡$SiOH^0$ sites, with the number of deprotonated surface groups, ≡SiO^-, increasing with an increasing pH. X-ray photoelectron spectroscopy indicates that the density of the ≡SiO^- sites is at a maximum at pH 8. Since a mixture of both ≡$SiOH^0$ and ≡SiO^- sites is available for ion sorption to the surface, MD simulations have examined trends in Ln(III) reactions with both types. The PMF of La(III) to the 001 surface of fully protonated α-quartz reveals a free-energy path for sorption that is repulsive using any of the potentials discussed above. An equilibrium simulation of trivalent La, in which the ion is first held at 3.0 or 2.0 Å above the average plane of the silanol O atoms, leads to immediate diffusion of $La(H_2O)_9^{3+}$ from the surface using the PCM derived potential. However, if the La(III) is able to penetrate closer to the quartz surface (equilibration at an initial distance of 1.0 Å), then the ion is able to coordinate to a silanol group and subsequently desorb with an attached −OH ligand. Note that the OH ligand is not strictly OH^- because the partial atomic charges on the O and H atoms lead to a net charge of −0.41 for the OH group that is transferred from the silanol to the ion.

Sorption to a ≡SiO^- site has a very different free-energy profile from that of sorption to a ≡$SiOH^0$ group. Using the gas-phase potential, both inner- and outer-sphere adsorbed species are indicated by the PMF (Figure 3). The outer-sphere complex, which has 9.1 waters of hydration in its first hydration shell, is predicted to exist at a distance of ∼5.5 Å and to have a free energy minimum of ∼−2.0 kcal/mol, whereas the inner-sphere species is sorbed at ∼3.2 Å from the average plane formed by the surface oxygens, having lost two waters of hydration during sorption and existing within a free energy minima of ∼−3.5 kcal/mol. The PCM-derived potential yields similar data, but with slightly more stability of the outer sphere sorbed species. Although these data were obtained with the SPC water model, it is anticipated that similar results will be obtained using water models that include static polarization effects, such as SPC/E. The lack of any polarization within the water model is likely the source of the small values for the free energy minima, and addition of polarization effects should increase the stability of the surface-bound species.

Equilibration simulations wherein the La(III) is initially placed 5.0 Å from the quartz surface yields a stable sorbed outer-sphere species. A preference for this outer-sphere complex is, however, indicated by the observation that when initially placed at 3.0 Å from the surface (near the minimum of the PMF for the inner-sphere species), the ion promptly migrates ∼1.5 Å farther from the surface and exists as an outer-sphere $La(H_2O)_9^{3+}$. If the ion is initially placed 2.0 or 1.0 Å from the surface plane, then inner-sphere species are observed wherein the La is coordinated to five waters of hydration with r_{La-OH_2} bond distances of 2.42−2.87 Å. The rest of the coordination shell of La(III) consists of one bond to the surface ≡SiO^- group (r_{La-O} = 2.2 Å), one bond to a surface ≡$SiOH^0$ group (r_{La-OH} = 2.3 Å), and two −OH ligands that have been transferred from the silica surface during equilibration. Those sites where −OH transferred from the surface are passivated by water migration to the defect. When using the La−OH_2 interaction potential from the solution-phase DFT data, similar results are observed for the simulations at initial distances of 2.0 and 1.0 Å; however, the average inner-sphere hydration number is 5.6, with an equilibrium being present between the inner-sphere sorbed species described above, and an inner-sphere species characterized by six waters of hydration, bound to one ≡SiO^-, one ≡$SiOH^0$, and one −OH ligand.

The predicted surface chemistry of Eu(III) is very similar to that of La(III). The PMF free energy profile to fully protonated quartz indicates that Eu(III) sorption is not favorable. If the ion is forced too close to the surface, an −OH group may transfer from the surface to the first solvation shell. The resulting species then desorbs from the surface, leaving an under-coordinated Si defect site. The PMF of Eu(III) sorption to a deprotonated site on quartz predicts both inner- and outer-sphere species. Similar to Figure 3, the latter has a minimum 5.2 Å from the average plane formed by the surface oxygens, having a full complement of 9.0 H_2O in its first hydration shell and with a predicted free energy of reaction of ∼−2.0 kcal/mol. The inner-sphere species is predicted to occur at a distance of 3.4 Å from the surface plane,

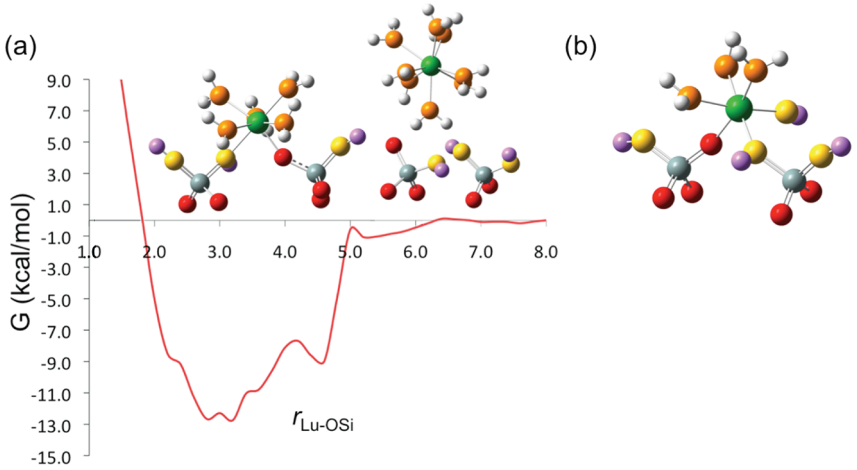

Figure 4. (a) PMF free-energy profile for Lu(III) sorption to quartz using the Lu−OH_2 interaction potential derived from gas phase DFT data, with structures of inner- and outer-sphere species inset. (b) Snapshot of sorbed Lu(III) on the surface of quartz from equilibrium simulation at an initial distance of 2.0 Å from the plane formed by the surface silanol O atoms. Si atoms colored gray; bridging O atoms are red; hydroxyl O atoms, yellow; hydroxyl H atom, pink; water O atoms are orange; water H atoms, white.

having lost two waters of hydration and existing within a free energy minimum of ∼−2.5 kcal/mol. A higher activation barrier is predicted for conversion between the inner- and outer-sphere species for sorbed Eu(III) (Figure S2 in the Supporting Information). Full equilibration of the presorbed inner-sphere ion at an initial distance of 3.0 Å predicts a stable outer sphere sorbed species; however, if the ion is initially placed at 2.0 Å, then an inner species is observed that is coordinated directly to the ≡SiO^- site. If the ion is pushed closer to the surface, and the equilibration begins at an initial distance of 1.0 Å, then the sorbed Eu(III) has six waters of hydration and is bound to one deprotonated surface ≡SiO^- group and one ≡$SiOH^0$ group and has the last open position in its coordination shell filled by an −OH group that has transferred from the silica surface.

In comparison with the experimental data for Eu(III) sorption to quartz at pH 7 and 9, the number of waters of hydration within the inner-sphere species bound to an ≡SiO^- site is in excellent agreement with presorbed equilibration at initial distances of 1.0 and 2.0 Å. Recall that extrapolation to zero ionic strength led to hydration numbers of surface-sorbed Eu(III) of 6.6 H_2O at pH 7.0 and 5.6 H_2O at pH 9.0. These theoretical data indicate that relative to the ideal 001 α-quartz surface used in the simulations, surface conditions within the experimental quartz dust may enable Eu(III) to approach the surface at a very close distance. Our results further indicate that sorption occurs only to deprotonated sites. The change in hydration number of inner-sphere species as a function of pH may be due to changes in surface charging, densities in adsorption sites (e.g., Ln(III) sorption to >1≡SiO^- group at a time), or the sorption of Eu-carbonate species (however, these would likely have fewer waters of hydration, since carbonate is generally a bidentate ligand). The decrease in the hydration number at pH 9 relative to pH 7 within the LIF studies more likely indicates participation of monodentate hydroxyl groups, a feature of the chemistry that is reflected within the MD studies wherein an −OH is observed to transfer from the silica surface to the first coordination sphere of Eu(III).

Moving across the period to Lu(III) results in chemistry significantly different from that predicted for La(III) and Eu(III) within the MD simulations. Within the protonated surface sorption MD simulations, the PMF predicts that no sorption should occur; however, if the Lu(III) is presorbed at 3.0, 2.0, or 1.0 Å, OH dissociation on the silica surface appears to stabilize inner-sphere Lu(III) species using either the gas phase or PCM-derived interatomic potentials. In some cases, the hydroxyl-bound aqueous Lu(III) desorbs toward the end of the third nanosecond of equilibration. According to the PMF, sorption to a deprotonated surface site using the gas phase fit Lu−OH_2 interaction potential results in an outer-sphere $Lu(H_2O)_8^{3+}$ species at 5.4 Å from the average plane formed by the surface oxygens, with a very small free energy of reaction (−1 kcal/mol).

A very strongly bound inner-sphere species is observed having 5.1−6 H_2O molecules of hydration and existing between 2.8 and 4.0 Å from the average plane formed by the surface oxygens within an energy well of −12.7 kcal/mol (Figure 4). The broad energy well for the inner-sphere species leads to a distribution of varying coordination environments for the Lu(III) species. A similar result is obtained for the PMF of Lu(III) using the Lu−OH_2 potential derived from the solution-phase DFT data; however, the well depth of the inner-sphere species is −6 kcal/mol. Thus, both interatomic potentials predict significantly stronger inner-sphere sorption of Lu(III) relative to La(III) and Eu(III). Equilibration of presorbed Lu(III) to the deprotonated site at an initial distance of 3.0 Å from the plane of the surface silanol groups results in a stable outer sphere sorbed species with a full complement of inner-shell solvating waters. If the equilibrations begin at sequentially closer distances to the surface, then a distribution of inner-sphere sorbed species is observed that have 3−5 waters of hydration in the first solvation shell of Lu(III) and binding at least one surface ≡SiO^- group and one ≡$SiOH^0$, with the remainder of the coordination environment filled out by −OH ligands that have transferred from the surface (Figure 4). These results agree well with experimental data that has indicated increasing sorption for Ln(III) ions to quartz at pH 7 and 9 across the 4f period (in the absence of precipitation).[63]

CONCLUSIONS

The present work has combined classical molecular dynamics and experimental sorption as well as laser-induced fluorescence

to determine the nature of sorbed trivalent lanthanide ions to the surface of α-quartz. These ions have been chosen because they are considered chemical analogues for An(III) but are not susceptible to redox reactions that can complicate their aqueous and surface reactivity. Given that quartz has a point-of-zero-charge of ~2.3, the surface is dominated by $\equiv SiOH^0$ sites, with the number of deprotonated surface groups, $\equiv SiO^-$, increasing with increasing pH. Thus, the MD simulations examined sorption of a single Ln(III) ion to both $\equiv SiOH$ and $\equiv SiO^-$ surface groups. The MD studies predict stronger sorption to the surface going from La(III) to Eu(III) to Lu(III), in agreement with the increasing surface charge density of the ions going across the lanthanide period. Although both inner- and outer-sphere species are observed in all cases, the potential of mean force studies indicate that the well depth for the inner-sphere sorbed cation increases significantly for Lu(III) relative to Eu(III).

A series of MD equlibrations were initiated at varying distances between the ion and the plane of the surface silanol O atoms. These studies reveal that if the ion is able to come within 2−3 Å of the surface plane, then reactivity may occur wherein surface −OH groups transfer from the silica and bind in the first coordination sphere of the lanthanide cation, forming a highly stable inner-sphere species. These data are particularly intriguing because the simulation surface studied within this work is the 001 face of α-quartz and free of any defects. Although the experimental quartz sample was verified to be α-quartz and the 001 face is the most prevalent under these experimental conditions, the presence of surface defects is virtually assured and may increase the possibility of a "close encounter" with Ln(III) that would facilitate the participation of surface hydroxyl reactivity. Sorption to a fully protonated surface is predicted to be unfavorable for all cations.

The redox stability of Ln(III) facilitates the experimental study of Eu(III) sorption at a number of ionic strengths, allowing the extrapolation of key data to zero ionic strength, and a more direct comparison with the data obtained by MD simulations. Sorption studies were performed at pH 7 and 9 to compare experimental and simulation data for Eu sorption to different potential surface sites. In comparison with the experimental data for Eu(III) sorption to quartz at pH 7 and 9, the numbers of waters of hydration within the inner-sphere species bound to an $\equiv SiO^-$ site are in excellent agreement. The decrease in the hydration number at pH 9 relative to pH 7 within the LIF studies may indicate possible participation of hydroxyl groups, a feature of the chemistry that is reflected within the MD studies (although the presence of surface carbonate species cannot be eliminated). Since the water model employed within the MD studies likely underestimates this type of reactivity, because no polarization effects are taken into account, the prevalence of the surface reactivity observed within the MD data in combination with the LIF data indicates a surface reaction mechanism that should be pursued in future work. Thus, the combined experimental and theoretical approach yields a self-consistent picture of trivalent lanthanide sorption to a quartz surface. Further, the extrapolation of experimental data to the zero ionic strength limit is a valuable tool toward a research goal of having direct comparisons between experimental and theoretical data.

■ ASSOCIATED CONTENT

Ⓢ Supporting Information. Detailed simulation protocols along with the final parameters obtained by fitting the Ln(III)−OH_2 interaction to the ab initio gradients for water dissociation. Experimental Eu(III) adsorption data on quartz at pH 7 and pH 9 as a function of ionic strength, *I*, in molarity. Fast and slow Eu(III) fluorescence decay constants in addition to the calculated number of waters of hydration at pH 7 and pH 9 as a function of ionic strength, *I*, in molarity. Complete references for both Gaussian03 and NWChem. This material is available free of charge via the Internet at http://pubs.acs.org.

■ AUTHOR INFORMATION

Corresponding Author

*E-mails: (A.E.C.) auclark@wsu.edu, (N.A.W.) nawall@wsu.edu, (Z.W.) zheming.wang@pnl.gov.

Present Addresses

§Department of Chemistry, Drexel University, Philadelphia, PA 19104.

■ ACKNOWLEDGMENT

This work was supported by the U.S. Department of Energy, Office of Nuclear Energy, Science and Technology, Junior Faculty Award Program award no. DE-FG07-05ID14692/IDNE006. This work was performed in part at the William R. Wiley Environmental Science Laboratory and using the Molecular Science Computing Facility (MSCF) therein, a national scientific user facility sponsored by the U.S. Department of Energy's Office of Biological and Environmental Research and located at the Pacific Northwest National Laboratory, operated for the Department of Energy by Battelle.

■ REFERENCES

(1) Choppin, G. R. *Marine Chem.* **1989**, *28*, 19–26.
(2) Raymond, K.; Szigethy, G. *Mater. Res. Soc. Symp. Proc.* 2008, *1104*, Paper no. 1104-NN04-01.
(3) Stumpf, S.; Srumpf, Th.; Lutzenkirchen, J.; Fanghanrl, Th. *J. Colloid Interface Sci.* **2008**, *318*, 5–14.
(4) Chung, K. H.; Klenz, R.; Park, K. K.; Paviet-Hartmann, P.; Kim, J. I. *Radiochim. Acta* **1998**, *82*, 215.
(5) Al-Abadleh, H. A.; Grassian, V. H. *Surf. Sci. Rep.* **2003**, *52*, 63–161.
(6) Katz, I. E.; Hayes, K. F. *J. Colloid Interface Sci.* **1995**, *170*, 477–490.
(7) Katz, I. E.; Hayes, K. F. *J. Colloid Interface Sci.* **1995**, *170*, 491–501.
(8) Kosmulski, M.; Sprycha, R.; Szczypa, J. *Surfactant Sci. Ser.* **2000**, *88*, 163–233.
(9) Brown, G. E., Jr.; Sturchio, N. C. *Rev. Mineral. Geochem.* **2002**, *49*, 1–115.
(10) Greathouse, J. A.; O'Brien, R. J.; Bemis, G.; Pabalan, R. T. *J. Phys. Chem. B* **2002**, *106*, 1646–1655.
(11) Hyun, S. P.; Cho, Y. H.; Hahn, P. S. *J. Colloid Interface Sci.* **2003**, *257*, 179–187.
(12) Lutzenkirchen, J. *J. Colloid Interface Sci.* **1997**, *195*, 149–155.
(13) Wu, Z.; Jun, L.; Hongyan, G. *Chem. Speciation Bioavailability* **2001**, *13*, 75–81.
(14) Stumm, W.; Hohl, D.; Dalang, F. *Croat. Chem. Acta* **1976**, *48*, 491–504.
(15) Kuta, J.; Clark, A. E. *Inorg. Chem.* **2010**, *49*, 7808–7817.
(16) Becke, A. D. *J. Chem. Phys.* **1993**, *98*, 5648–5652.
(17) Lee, C.; Yang, W.; Parr, R. G. *Phys. Rev. B* **1988**, *37*, 785–789.
(18) Dolg, M.; Stoll, H.; Preuss, H. *J. Chem. Phys.* **1989**, *90*, 1730–1734.
(19) Cao, X.; Dolg, M. *J. Mol. Struct. (THEOCHEM)* **2002**, *581*, 139–147.

(20) Dunning, T, H., Jr. *J. Chem. Phys.* **1989**, *90*, 1007.
(21) Bylaska, E. J. et al. *NWChem, A Computational Chemistry Package for Parallel Computers*; Version 5.1, Pacific Northwest National Laboratory, Richland, WA 99352-0999, USA, 2007 (see the Supporting Information for complete reference).
(22) Barone, V.; Cossi, M.; Tomasi, J. *J. Chem. Phys.* **1997**, *107*, 3210–3221.
(23) Gaussian 03, Revision C.02, Frisch, M. J. et al. Gaussian, Inc., Wallingford CT, 2004 (see the Supporting Information for complete reference).
(24) Waldher, B.; Kuta, J.; Chen, S.; Henson, N.; Clark, A. E. *J. Comput. Chem.* **2010**, *31*, 2307–2316.
(25) ForceFit download: http://aclark.chem.wsu.edu/software.
(26) Berendsen, H. J. C.; Postma, J. P. M.; van Gunsteren, W. F.; Hermans, J. In *Intermolecular Forces*; Pullman, B., Ed.; Kluwer: Boston, 1981.
(27) Teleman, O.; Jonsson, B.; Engstrom, S. *Mol. Phys.* **1987**, *60*, 193–203.
(28) Wallqvist, A.; Teleman, O. *Mol. Phys.* **1991**, *74*, 515–533.
(29) Duvail, M.; Spezia, R.; Cartailler, T.; Vitorge, P. *Chem. Phys. Lett.* **2007**, *448*, 41–45.
(30) Hagberg, D.; Karlstrom, G.; Roos, B. O.; Gagliardi, L. *J. Am. Chem. Soc.* **2005**, *127*, 14250.
(31) Spohr, E.; Palinkas, G.; Heinzinger, K.; Bopp, P.; Probst, M. M. *J. Phys. Chem.* **1988**, *92*, 6754.
(32) Todorov, I. T.; Smith, W.; Trachenko, K.; Dove, M. T. *J. Mater. Chem.* **2006**, *16*, 1911–1918.
(33) Wander, M. C. F.; Clark, A. E. *J. Phys. Chem. C* **2008**, *112*, 19986–19994.
(34) Plimpton, S. J. *J. Comput. Phys.* **1995**, *117*, 1–19.
(35) LAMMPS download: http://lammps.sandia.gov
(36) Cygan, R. T.; Liang, J.-J.; Kalinichev, A. G. *J. Phys. Chem. B* **2004**, *108*, 1255–1266.
(37) Kohler, M.; Curtis, G. P.; Kent, D. B.; Davis, J. A. *Water Resour. Res.* **1996**, *32*, 3539–3551.
(38) Chenchen, C.; Coleman, M.; Katz, L. *Environ. Sci. Technol.* **2006**, *40*, 142.
(39) Shannon, R. D. *Acta Crystallogr.* **1976**, *A32*, 751–767.
(40) Allen, P. G.; Bucher, J. J.; Dhuh, D. K.; Edelstein, N. M.; Craig, I. *Inorg. Chem.* **2000**, *39*, 595–601.
(41) Cossy, C.; Helm, L.; Powell, D. H.; Merbach, A. E. *New J. Chem.* **1995**, *19*, 27–35.
(42) Habenschuss, A.; Spedding, F. H. *J. Chem. Phys.* **1979**, *70*, 2797–2806.
(43) Habenschuss, A.; Spedding, F. H. *J. Chem. Phys.* **1979**, *70*, 3758–3763.
(44) Habenschuss, A.; Spedding, F. H. *J. Chem. Phys.* **1980**, *73*, 442–450.
(45) Ouerfelli, N.; Ammar, M.; Latrous, H. J. *Chim. Phys.* **1994**, *91*, 1786.
(46) Latrous, H.; Oliver, J. *J. Mol. Liq.* **1999**, *81*, 115.
(47) Floris, F. M.; Tani, A. *J. Chem. Phys.* **2001**, *115*, 4750.
(48) Näslund, J.; Lindqvist-Reis, P.; Persson, I.; Sandström, M. *Inorg. Chem.* **2000**, *39* (18), 4006–4011.
(49) Choppin, G. R.; Wang, Z. M. *Inorg. Chem.* **1997**, *36*, 249–252.
(50) Yamaguchi, T.; Nomura, M.; Wakita, H.; Ohtaki, H. *J. Chem. Phys.* **1988**, *89* (8), 5153–5159.
(51) Guillaumont, R.; Fanghanel, T.; Volker, N.; Fuger, J.; Palmer, D. A.; Grenthe, I.; Rand, M. H. *Update on the Chemical Thermodynamics of Uranium, Neptunium, Plutonium, Americium and Technetium*; Elsevier: Issy-les_Moulineaux, France, 2003.
(52) Carnall, W. T.; Fields, P. R.; Rajnak, K. *J. Chem. Phys.* **1968**, *49*, 4450–4455.
(53) Bunzli, J. C. G.; Yersin, J. R. *Inorg. Chem.* **1979**, *18*, 605–607.
(54) Ozaki, T.; Arisaka, M.; Kimura, T.; Francis, A. J.; Yoshida, Z. *Anal. Bioanal. Chem.* **2002**, *374*, 1101–1104.
(55) Richardson, F. S. *Chem. Rev.* **1982**, *82*, 541–552.
(56) Tan, X. L.; Wang, X. K.; Geckeis, H.; Rabung, Th. *Environ. Sci. Technol.* **2008**, *42*, 6532–6537.3.
(57) Horrocks, W. D., Jr.; Albin, M. In *Progress in Inorganic Chemistry*; Lippard, S. J, Ed.; Wiley & Sons: New York, 1984.
(58) Wang, Z.; Felmy, A. R.; Xia, Y.; Qafoku, O.; Yantasee, W.; Cho, H. M. *Radiochim. Acta* **2005**, *93*, 741–748.
(59) Wang, Z.; van der Burt, L. J.; Choppin, G. R. *Inorg. Chim. Acta* **1999**, *293*, 167–177.
(60) Wang, Z. Spectroscopic studies of lanthanide complexes with organic ligands. Ph. D. Dissertation, Florida State University, Tallahassee, FL, 1994.
(61) Blasse, G. *Prog. Solid State Chem.* **1988**, *18*, 79–171.
(62) Duval, Y.; Mielczarski, J. A.; Pokrovsky, O. S.; Mielszarski, E.; Ehrhardt, J. J. *J. Phys. Chem. B.* **2002**, *106*, 2937–2945.
(63) Perelomov, L. V.; Yoshida, S. *Water Air Soil Pollut.* **2008**, *194*, 217–225.